INSTITUTE OF PHYSICS PUBLISHING SUPERCONDUCTOR SCIENCE AND TECHNOLOGY

Supercond. Sci. Technol. **17** (2004) S127–S131 PII: S0953-2048(04)72363-5

A superconducting phase-locked local oscillator for a submillimetre integrated receiver

V P Koshelets[1,3], S V Shitov[1,3], L V Filippenko[1], P N Dmitriev[1], A B Ermakov[1,3], A S Sobolev[1], M Yu Torgashin[1], A L Pankratov[2], V V Kurin[2], P Yagoubov[3] and R Hoogeveen[3]

[1] Institute of Radio Engineering and Electronics (IREE), Mokhovaya 11, Bldg. 7, Moscow, 125009, Russia
[2] Institute for Physics of Microstructure (IPM), Ulyanov 46, GSP-105, Nizhny Novgorod, 603600, Russia
[3] National Institute for Space Research (SRON), Landleven, 12, PO Box 800, Groningen, 9700 Av., The Netherlands

Received 29 September 2003
Published 19 February 2004
Online at stacks.iop.org/SUST/17/S127 (DOI: 10.1088/0953-2048/17/5/007)

Abstract
Comprehensive measurements of the flux flow oscillator (FFO) radiation linewidth are performed using an integrated harmonic SIS mixer; the FFO linewidth and spectral line profile are compared to a theory. An essential dependence of the FFO linewidth on frequency is found; a possible explanation is proposed. The results of the numerical solution of the perturbed sine–Gordon equation qualitatively confirm this assumption. To optimize the FFO design, the influence of the FFO parameters on the radiation linewidth is studied. A novel FFO design at a moderate current density has resulted in a free-running FFO linewidth of about 10 MHz in the flux flow regime up to 712 GHz, limited only by the gap frequency of Nb. This relatively narrow free-running linewidth (along with implementation of a wide-band phase locking loop system) allows continuous phase locking of the FFO in the wide frequency range of 500–710 GHz. These results are the basis for the development of a 550–650 GHz integrated receiver for the terahertz limb sounder (TELIS) intended for atmosphere study and scheduled to fly on a balloon in 2005. We report here also on the design of the second generation of the phase-locked superconducting integrated receiver chip for TELIS.

(Some figures in this article are in colour only in the electronic version)

1. Introduction

At present a Josephson flux flow oscillator (FFO) [1] appears to be the most developed superconducting local oscillator for integration with an SIS mixer in a single-chip submillimetre wave receiver [2]. A superconducting integrated receiver (SIR) [2] comprises in one chip a planar antenna and an SIS mixer, pumped by an integrated superconducting local oscillator (LO). The concept of an SIR has been experimentally proven: a DSB receiver noise temperature below 100 K has been demonstrated around 500 GHz; a compact imaging array of nine SIRs has been developed and tested [2, 3]. The frequency resolution of a heterodyne spectrometer is one of the major parameters for a practical application. In order to obtain the required resolution (of at least one part per million) the local oscillator must be phase-locked to an external reference. To ensure the phase locking, the free-running linewidth of the FFO has to be well below an effective regulation bandwidth of the PLL (of about 10 MHz).

Detailed measurements of the FFO linewidth were performed in a wide frequency range up to 700 GHz using a novel experimental technique based on an integrated harmonic mixer [4]. A Lorentzian shape of the FFO line has been observed both at higher voltages on the flux flow step (FFS)

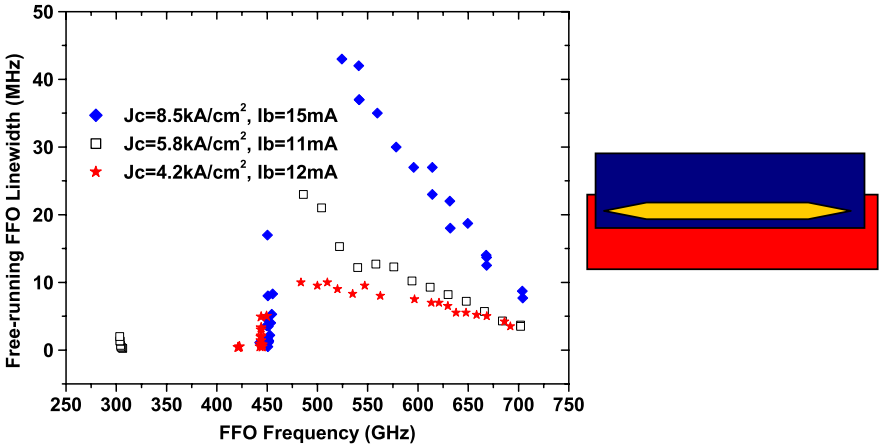

Figure 1. The dependence of the FFO linewidth on the oscillation frequency measured for FFOs of the same design (see the inset), but fabricated from three trilayers with different current densities, J_c. The linewidth is measured at constant bias current, while the FFO frequency (voltage) is tuned by the magnetic field (by the control line current).

and at lower voltages in the resonant regime on the Fiske steps (FSs) [5]. This means that the free-running ('natural') FFO linewidth in all operational regimes is determined by the wide-band thermal fluctuations and the shot noise. This is different from the case for many traditional microwave oscillators where the 'natural' linewidth is very small and the observed linewidth can be attributed mainly to external fluctuations. It was found [3–6] that the free-running FFO linewidth, δf, exceeds theoretical estimations made for a lumped tunnel Josephson junction. To explain the experimentally measured dependence of the FFO linewidth, an additional term proportional to the differential resistance on the control line current, R_d^{CL} (producing a magnetic field for the FFO operation), has been introduced to the noise model of the FFO [5–7]: $\delta f = (2\pi/\Phi_0^2)(R_d + K * R_d^{CL})^2 S_i(0)$; where $S_i(0)$ is the power density of the low frequency current fluctuations, R_d is the differential resistance on the bias current. Recently a physical reason for such an additional term has been proposed [8]. The solution is based on the assumption that part of the DC bias current creates an additional magnetic field in the junction.

In this report the results of a comprehensive study of the dependence of the FFO linewidth on the voltage (FFO frequency), the current density and the FFO geometry are presented. Section 3 of the paper is devoted to the design of and test results for the SIR with a phase-locked FFO designed for TELIS.

2. FFO linewidth; the dependence of the FFO frequency and current density

Experimentally measured dependences of the FFO linewidth are presented in figure 1 for junctions with uniform bias current distributions (without an 'unbiased tail'). The abrupt increase of the linewidth at the FFO frequency of about 450 GHz is caused by the effect of Josephson self-coupling (JSC) [9, 10], which considerably modifies the FFO properties at voltages $V \approx V_{JSC} = (1/3)V_{gap}$ (V_{JSC} corresponds to 450 GHz for an Nb–AlO_x–Nb FFO). This increase of the intrinsic FFO linewidth due to the larger internal damping caused by the JSC effect at voltages $V > V_{JSC}$ significantly complicates the phase locking of the FFO.

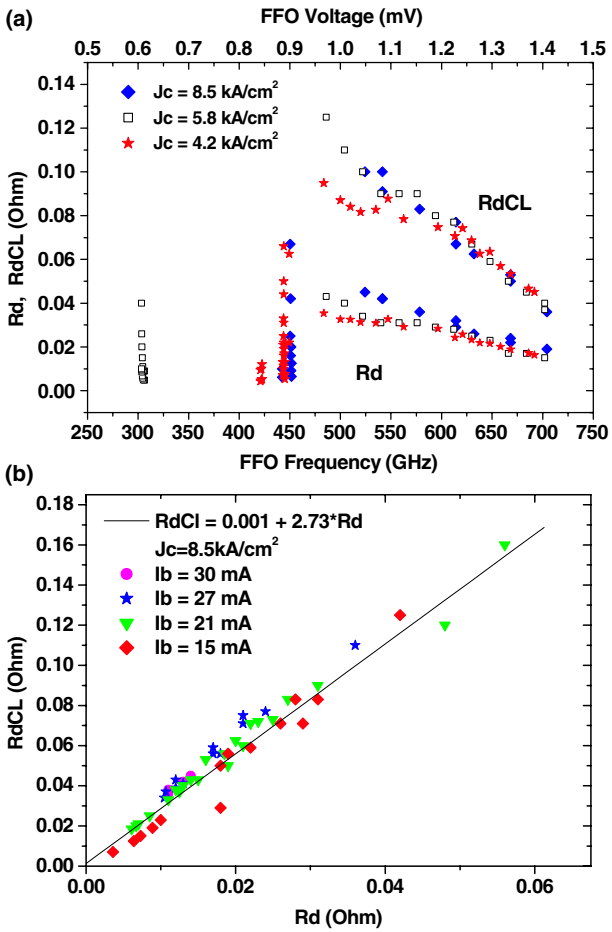

Figure 2. Differential resistances to the bias current, R_d, and magnetic field (control line current), R_d^{CL} versus the FFO frequency (a); and the dependence of R_d^{CL} on R_d (b). Differential resistances are calculated from the voltage change ΔV found upon a small incrementation of two currents, ΔI and ΔI_{cl}. The voltage change ΔV is determined by measuring the frequency of the emitted radiation.

For all current densities there is a well-defined dependence of the free-running FFO linewidth on the frequency (voltage).

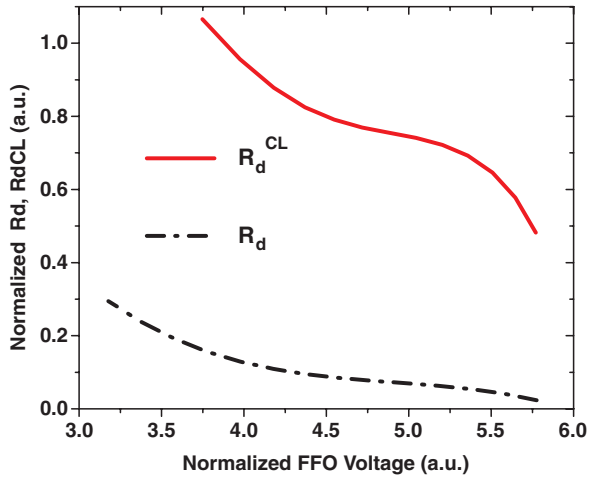

Figure 3. Differential resistances R_d and R_d^{CL} calculated at the normalized bias current 0.3 for the junction length $l = 40$ and damping $\alpha = 0.05$. The curves in the figure are the results of polynomial fitting to numerically calculated data.

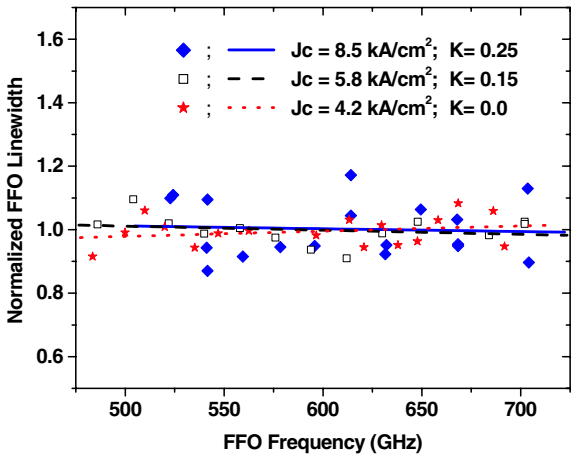

Figure 4. The experimental linewidth normalized to theoretical values. Calculations are based on the FFO model [5, 6] using experimentally measured values of differential resistances and currents. Linear fits to the normalized data are shown by appropriate lines.

In the model [5, 6] the direct voltage dependence of the FFO linewidth is negligibly small. Since the data are taken at a constant bias current, the variation of the linewidth with the bias voltage can be mainly attributed to changes in the differential resistance. Indeed, data in figure 2(a) demonstrate such a dependence (see also [11]); it is observed for all FFOs tested, of very different designs. It should also be mentioned that R_d and R_d^{CL} are bounded: their ratio is almost constant over the wide voltage range (see figure 2(b)). Presumably the dependence of R_d and R_d^{CL} on the FFO frequency (voltage) reflects the fact that introduction of an additional fluxon into the junction requires a larger control line current as the fluxon chain gets denser. This assumption is confirmed by numerical calculations (see figure 3).

It should be mentioned that the differential resistances for figure 2 were obtained during FFO linewidth measurements, which enables measurement of voltage increments with accuracy better than 20 nV by observing the frequency change of the emitted radiation. Note that the results of direct DC measurements (which average data in the range of about 1–2 μV) give exactly the same dependence.

The results of preliminary numerical solution of the perturbed sine–Gordon equation are presented in figure 3. The dimensionless parameters are chosen to be close to the experimental ones: the length (normalized to the Josephson penetration depth) $l = 40$, the damping $\alpha = 0.05$, the magnetic field varies from 3 to 8 (flux flow step). For so small a damping, the results of numerical calculations are 'noisy', so the polynomial fits to the data are presented in figure 3. As is seen from figure 3 both R_d^{CL} and R_d decrease with increase of the voltage.

Data presented in figure 1 demonstrate also a considerable increase of the FFO linewidth with FFO current density. Note that bias currents for all current densities are quite similar and their difference cannot explain the broadening of the FFO linewidth. Again, the increase is mainly caused by changing the differential resistance and can be quantitatively calculated from the model [5, 6]. This is confirmed by data presented in figure 4, where the experimental linewidth is normalized to theoretically calculated linewidth values. The linear fits to the normalized data coincide well with each other (and with the unity line) for all current densities. This proves that an additional broadening discussed in the papers [12, 13] does not play a significant role for the present FFO parameters and the linewidth can be precisely calculated using the FFO model developed [5–7]. Note that experimentally determined values of the coefficient K are used for the calculation of the FFO linewidth. This coefficient accounts for the influence of the magnetic field created by the bias current [8] by adding the product $K R_d^{CL}$ to the measured R_d. The K-value varies from 0.35 (at small bias currents near the quasiparticle curve) down to zero (at the end of the flux flow step) for the FFO without an 'unbiased tail'.

It has to be noted that high current density ($J_c \geqslant 8$ kA cm^{-2}) is important for wide-band operation of an SIS mixer at the submillimetre wave range. It is found that increase of the current density leads to growth of the differential resistances (instead of the expected decrease!) which creates serious problems in the design and development of SIR chips. Implementation of two separate trilayers with different current densities for the SIS mixer (high J_c) and for the FFO (lower J_c) might be the solution.

To study the dependence of the FFO linewidth on the profile of the bias current, we fabricated a set of FFOs with different numbers of separate bias 'fingers'. The FFO junction itself (i.e. the tunnel layer area) is exactly the same as in previous experiments (figures 1 and 2); only the geometry of the top electrode is changed. Each 'finger' (width—4 μm, separation between fingers—16 μm) includes a small series resistor to provide a uniform current distribution. Two schematic layouts of the tested circuits are shown in the right part of figure 5; for the layout with the 'unbiased tail', parts of the 'fingers' from the input end (shown by a different shade) were removed. Our measurements demonstrate that the design with separate fingers results in a much wider FFO linewidth (see figure 5—diamonds). For an FFO with an unbiased tail (several fingers from the 'input' end of the FFO are removed) the linewidth becomes smaller, approaching the

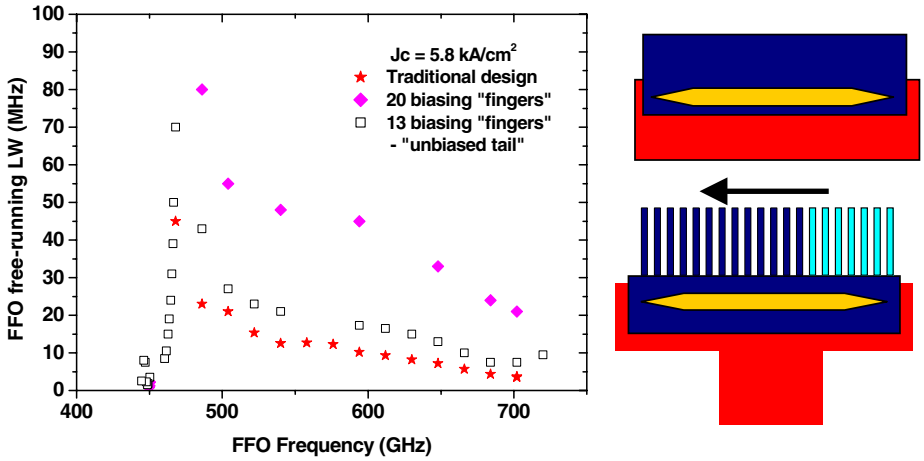

Figure 5. The experimental linewidth measured for FFOs of different design. Schematic sketches for two tested designs are shown as insets.

data for the traditional design, which can be described as one broad electrode, not divided into 'fingers'. The reason for the essential increasing of the FFO linewidth for a biasing scheme with separate fingers might be the spatial modulation of the bias current. In the case of an 'unbiased tail' such modulation is applied far from the input end. These data demonstrate that the linewidth of the oscillator is mainly determined by the processes at the 'input' end of the FFO. Additional studies are required for optimization of the FFO design for TELIS.

3. Design and testing of the phase-locked SIR

In order to resolve a weak signal adjacent to a strong spectral line, a local oscillator of a heterodyne spectrometer (PL FFO) must have a well-defined (narrow) line-shape. The dynamic range of the spectrometer is closely related to the ratio between the carrier and the spectral power density (FFO phase noise) at a frequency offset equivalent to the channel spacing of the spectrometer. A phase noise of the phase-locked FFO of about -80 dBc Hz^{-1} at the 1 MHz offset from the carrier has been reported at 700 GHz [14]. For the 1 MHz channel one may expect a dynamic range of 20 dB for the spectrometer that satisfies the requirements for single-dish radio astronomy and atmospheric monitoring. For comparison, this figure meets well the requirements for the wide-band spectrometer of the HIFI instrument of the Herschel Space Observatory prepared for launch in 2007.

We have demonstrated experimentally for the first time a sensitive heterodyne spectrometer employing a superconducting local oscillator at 327 GHz [15]. A breadboard of a superconducting integrated spectrometer with the phase-locked FFO has been tested, showing frequency resolution of the receiver as good as 10 kHz. The effect of the broadening of a spectral line of SO_2 gas at 326 867 MHz was measured using this spectrometer for a laboratory gas cell within the pressure range of 0.03–0.3 mbar, demonstrating the feasibility of using such a device in practical applications.

Here we report on the first results of design and testing of the phase-locked SIR for TELIS. The device comprises a double-dipole lens–antenna SIS mixer pumped by an integrated FFO. The FFO provides the rf power also for the harmonic mixer integrated on the same silicon chip of size

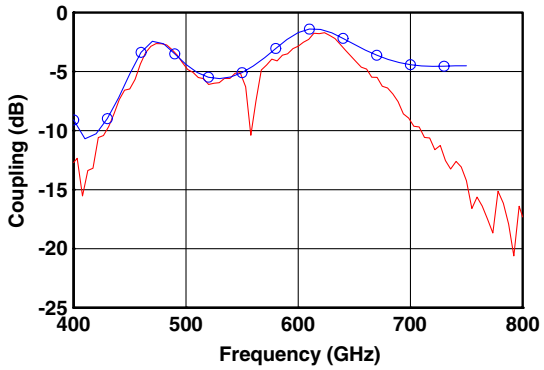

Figure 6. Experimental FTS data (solid) and a simulated fit (smooth curve marked by circles) for signal coupling for the twin-SIS double-dipole mixer. The increasing discrepancy above 670 GHz is caused by dissipative loss above the gap frequency of Nb. The dips in the measure spectral response (FTS data) are water absorption lines.

4 mm $\times$ 4 mm $\times$ 0.3 mm; this harmonic mixer is a part of the FFO phase locking loop. Since the advantage of the SIR technology is the wide-band tunability of the integrated FFO, we are developing a new wide-band device with an instantaneous bandwidth of 500–650 GHz emphasizing the 600–650 GHz frequency range. This enables covering the wide range of atmospheric species responsible for ozone depletion. A few new solutions are implemented in the SIR chip, making it a new generation device. To achieve the wide-band performance of the spectrometer, a side-feed twin-SIS mixer with 0.8 μm^2 junctions integrated with a double-dipole antenna is used. To minimize the magnetic field interference to the FFO, the control line of the SIS mixer (the integrated magnetic coil) is folded and placed opposite to the FFO, resulting in a 10^{-3} suppression coefficient.

A few batches have already been produced at IREE and preliminary testing has been done at SRON at dc and with a Fourier transform spectrometer (FTS). The FTS test presented in figure 6 demonstrates the possibility of obtaining a wide instantaneous bandwidth for the double-dipole twin-SIS mixer. However, we did not succeed in getting precise wide-band and low loss coupling over the complete band. The fit demonstrated in figure 6 is only a qualitative one. Analysing the experimental

data, we have found that accurate EM simulation of the antenna structure is required. A few important results have been obtained recently via development of proper EM models for the key elements of the circuit; this provides a good basis for further improvement of the complex SIR device. A heterodyne test is in preparation.

Acknowledgments

The work was supported in parts by RFBR (projects 03-02-16748, 02-02-16775, 03-02-16533, 03-02-06343, 03-02-06683), by INTAS (project 01-0367, 01-0450) and by ISTC project 2445.

References

[1] Nagatsuma T, Enpuku K, Irie F and Yoshida K 1983 *J. Appl. Phys.* **54** 3302–9
See also, Nagatsuma T, Enpuku K, Irie F and Yoshida K 1984 *J. Appl. Phys.* **56** 3284 Part II
Nagatsuma T, Enpuku K, Irie F and Yoshida K 1985 *J. Appl. Phys.* **58** 441 Part III
Nagatsuma T, Enpuku K, Irie F and Yoshida K 1988 *J. Appl. Phys.* **63** 1130 Part IV

[2] Koshelets V P and Shitov S V 2000 *Supercond. Sci. Technol.* **13** R53–69

[3] Shitov S V, Koshelets V P, Ermakov A B, Filippenko L V, Baryshev A M, Luinge W and Gao J-R 1999 *IEEE Trans. Appl. Supercond.* **9** 3773–6

[4] Koshelets V P, Shitov S V, Filippenko L V, Shchukin A V and Mygind J 1996 *Appl. Phys. Lett.* **69** 699–701

[5] Koshelets V P, Ermakov A B, Dmitriev P N, Sobolev A S, Baryshev A M, Wesselius P R and Mygind J 2001 *Supercond. Sci. Technol.* **14** 1040–3

[6] Koshelets V P, Dmitriev P N, Sobolev A S, Khodos V V, Pankratov A L, Vaks V L, Baryshev A M, Wesselius P R and Mygind J 2002 *Physica* C **372–376** 316–21

[7] Pankratov A L 2002 *Phys. Rev.* B **65** 054504

[8] Mygind J, Mahaini C, Samuelsen M R, Sobolev A S, Torgashin M Y and Koshelets V P 2004 Spectral linewidth of Josephson flux flow oscillators; influence from bias and geometry *Supercond. Sci. Technol.* submitted

[9] Hasselberg L-E, Levinsen M T and Samuelsen M R 1974 *Phys. Rev.* B **9** 3757–65

[10] Koshelets V P, Shitov S V, Shchukin A V, Filippenko L V, Mygind J and Ustinov A V 1997 *Phys. Rev.* B **56** 5572–7

[11] Koshelets V P, Shitov S V, Dmitriev P N, Ermakov A B, Sobolev A S, Torgashin M Yu, Wesselius P R, Yagoubov P A, Mahaini C and Mygind J 2003 *IEEE Trans. Appl. Supercond.* **13** 1035–8

[12] Golubov A A, Malomed B A and Ustinov A V 1996 *Phys. Rev.* B **54** 3047

[13] Betenev A P and Kurin V V 1997 *Phys. Rev.* B **56** 7855

[14] Koshelets V P, Dmitriev P N, Ermakov A B, Sobolev A S, Torgashin M Yu, Khodos V V, Vaks V L, Wesselius P R, Mahaini C and Mygind J 2002 *Proc. 13th Int. Symp. on Space Terahertz Technology (Harvard University, 2002)* pp 473–82

[15] Shitov S V, Koshelets V P, Ermakov A B, Dmitriev P N, Filippenko L V, Khodos V V, Vaks V L, Yagoubov P A, Vreeling W-J and Wesselius P R 2003 *IEEE Trans. Appl. Supercond.* **13** 684–7